Original Paper

Cells Tissues Organs

Cells Tissues Organs 2012;196:523–533
DOI: 10.1159/000337490

Accepted after revision: February 13, 2012
Published online: July 10, 2012

Comparison of Platelet-Rich Plasma and VEGF-Transfected Mesenchymal Stem Cells on Vascularization and Bone Formation in a Critical-Size Bone Defect

P. Kasten[a, b] M. Beverungen[a, c] H. Lorenz[a] J. Wieland[c] M. Fehr[d] F. Geiger[a, e]

[a]Division of Experimental Orthopaedics, Orthopaedic University Hospital of Heidelberg, Heidelberg, [b]Department of Orthopaedic Surgery, University of Dresden, Dresden, [c]Harlan Cytotest Cell Research GmbH, Rossdorf, [d]Veterinary Medical Faculty Hannover, University of Hannover, Hannover, and [e]Orthopaedic University Hospital Friedrichsheim, University of Frankfurt, Frankfurt/Main, Germany

Key Words

Bone formation · Tissue engineering · Angiogenesis · Bone substitutes · Vascular endothelial growth factor · Osteogenesis · Mesenchymal stem cells · Gene therapy

Abstract

Both platelet-rich plasma (PRP) and vascular endothelial growth factor (VEGF) can promote regeneration. The aim of this study was to compare the effects of these two elements on bone formation and vascularization in combination with bone marrow stromal cells (BMSC) in a critical-size bone defect in rabbits. The critical-size defects of the radius were filled with: (1) a calcium-deficient hydroxyapatite (CDHA) scaffold + phVEGF$_{165}$-transfected BMSC (VEGF group), (2) CDHA and PRP, or (3) CDHA, autogenous BMSC, and PRP. As controls served: (4) the CDHA scaffold alone and (5) the CDHA scaffold and autogenous BMSC. The volume of new bone was measured by means of micro-CT scans, and vascularization was assessed in histology after 16 weeks. Bone formation was higher in the PRP + CDHA, BMSC + CDHA, and PRP + BMSC + CDHA groups than in the VEGF group ($p < 0.05$). VEGF transfection significantly promoted vascularization of the scaffolds in contrast to BMSC and PRP ($p < 0.05$), but was similar to the result of the CDHA + PRP + BMSC group. The results show that VEGF-transfected BMSC as well as the combination of PRP and BMSC improve vascularization, but bone healing was better with the combination of BMSC and PRP than with VEGF-transfected BMSC. Expression of VEGF in BMSC as a single growth factor does not seem to be as effective for bone formation as expanded BMSC alone or PRP which contains a mixture of growth factors.

Abbreviations used in this paper

μ-CT	micro-computer tomography
BMSC	bone marrow stromal cells
CDHA	calcium-deficient hydroxyapatite
ECGF	epithelial cell growth factor
EGF	epidermal growth factor
FCS	fetal calf serum
IGF	insulin-like growth factor
NZWR	New Zealand white rabbits
PBS	phosphate-buffered saline
PDGF	platelet-derived growth factor
PRP	platelet-rich plasma
TGF	transforming growth factor
VEGF	vascular endothelial growth factor

KARGER

Fax +41 61 306 12 34
E-Mail karger@karger.ch
www.karger.com

1422–6405/12/1966–0523$38.00/0

Accessible online at:
www.karger.com/cto

Priv.-Doz. Dr. Florian Geiger
Orthopaedic University Hospital Friedrichsheim
J.W. Goethe Universität Frankfurt
Marienburgstrasse 2, DE–60528 Frankfurt (Germany)
Tel. +49 69 6705 408, E-Mail florian.geiger@friedrichsheim.de

Introduction

Healing large bone defects remains a major challenge in orthopedic surgery [Damien and Parsons, 1991; Arrington et al., 1996]. As autogenously harvested bone transplants are limited and callus distraction is not feasible in every defect site, alternative strategies involving the use of bone substitutes, bone marrow stromal cells (BMSC), and growth factors have successfully been explored [Niemeyer et al., 2009a, b; Janicki et al., 2010; Kasten et al., 2010]. It is known that vascularization is important and tightly regulated in bone healing [DePalma et al., 1972; Burchardt and Enneking, 1978]. Healing occurs in three distinct but overlapping stages: (1) the early inflammatory stage, (2) the repair stage, and (3) the late remodeling stage [Bruder et al., 1994]. In the inflammatory stage of the first weeks the ingrowth of vascular tissue takes place and improves the nutrient and oxygen supply [DePalma et al., 1972; Burchardt and Enneking, 1978]. During the repair stage, fibroblasts begin to lay down a stroma that helps support vascular ingrowth [Laurencin et al., 1999]. As vascular ingrowth progresses, a collagen matrix is laid down while osteoid is secreted and subsequently mineralized, which leads to the formation of a soft callus around the repair site [DePalma et al., 1972; Burchardt and Enneking, 1978]. Fracture healing is completed during the remodeling stage in which the healing bone is restored to its original shape, structure, and mechanical strength. During this stage a stable and sufficient vascular supply is formed.

As vascularity of the healing site is important during all stages, growth factors that improve vascularity have become increasingly popular. Vascular endothelial growth factor (VEGF), for example, has proven to increase the blood supply [Geiger et al., 2007a]. The short half-life of VEGF (6–8 h), however, is considered problematic to achieve an effective level of growth factors. Therefore, a steady level of growth factor release at the site of the bony defect by viral transfection of BMSC has been investigated in the past [Geiger et al., 2007a]. Indeed, transfection of BMSC by the mammalian expression vector phVEGF$_{165}$ which contains the cDNA for recombinant human VEGF$_{165}$ led to higher vascularization and faster resorption of the bone substitute [Geiger et al., 2007a]. Another adjunct to improve bone healing is platelet-rich plasma (PRP) [Kasten et al., 2008a; Niemeyer et al., 2010]. PRP can easily be obtained on the day of surgery by two centrifugation steps from autogenous whole blood. It contains not only VEGF but also a number of other growth factors like platelet-derived growth factor (PDGF), transforming growth factor (TGF)-β_1, TGF-β_2, insulin-like growth factor (IGF), epidermal growth factor (EGF), and endothelial cell growth factor (ECGF) in their natural composition [Kiuru et al., 1991; Kasten et al., 2006; Vogel et al., 2006]. A critical-size bone defect can heal if, for example, bone substitutes are inserted into the defect [Puelacher et al., 1996; Marcacci et al., 1999; Wippermann et al., 1999]. In the present study a resorbable synthetic bone substitution material called calcium-deficient hydroxyapatite (CDHA) was chosen as a scaffold whose surface area is approximately 50 m^2/g, thus approaching the values of about 80 m^2/g found in natural bone [Kasten et al., 2003].

The two aforementioned concepts for improving bone healing (on one hand gene therapy with the use of transfected BMSC and on the other hand the use of a mix of natural growth factors from platelets) are completely different, and research groups often use either one or the other. The aim of this study was to compare these two concepts in terms of efficacy in one experimental setting in a critical-size bone defect of the radius in rabbits. The hypothesis was that both concepts are equally effective in improving vascularization and finally bone healing.

Material and Methods

Animals

According to the study protocol, the following groups (each n = 6) were compared: The critical-size defects of the radius were filled with: (1) a CDHA scaffold + phVEGF$_{165}$-transfected BMSC (VEGF group), (2) CDHA and PRP, or (3) CDHA, autogenous BMSC, and PRP. As controls served: (4) the CDHA scaffold alone and (5) the CDHA scaffold and autogenous BMSC. Six- to 9-month-old female New Zealand white rabbits (NZWR) were kept in separate cages; they were fed a standard diet and allowed to move freely during the study. Animals were treated in compliance with our institution's guiding principles 'in the care and use of animals'. The local ethics committee for animal experiments approved the design of the experiment. The groups PRP + CDHA and PRP + BMSC + CDHA that were treated in parallel were used for comparison [Kasten et al., 2008b]. One animal in the CDHA + PRP group sustained a fracture of the forearm and was excluded from the study.

Ceramic Scaffolds and PRP

CDHA ceramic cylinders 15 mm in length and 4 mm in diameter [Dr. h.c. Robert Mathys Foundation (RMS), Switzerland] were produced in an emulsion process as described earlier [Bohner, 2000; LeGeros, 2002]. They have a specific surface area that approximates 48 m^2/g with a total porosity or 85 vol% (54% macropores and 31% micropores). As published previously, for the preparation of PRP, on average 17 ml (SD 3.67) of blood was ob-

tained from the ear arteries of six anesthetized 6-month-old NZWR [Kasten et al., 2008b]. The protocol was adapted from Yamada et al. [2004]. The blood was collected in tubes that were rinsed with heparin and the platelets were counted in Neugebauer chambers. The average platelet number was 1.9×10^8/ml (SD 0.39×10^8). Then, the blood was centrifuged twice: initially at 209 *g* for 16 min at 20°C to remove red blood cells and then at 1,500 *g* for 12 min at 20°C to obtain the platelet pellet. The cell pellet was suspended in platelet-poor plasma, resulting in an average platelet number of 10.05×10^8/ml (SD 3.2×10^8). The PRP of the six donors was mixed and stored at –80°C until needed, and consequently allogenic and standardized PRP was used.

Bone Marrow Aspiration and BMSC Expansion

Bone marrow was aspirated and prepared from tibias from all rabbits about 18 days before surgery as described previously [Louisia et al., 1999]. In brief, the surgical technique was as follows: with the animal under general anesthesia, the bone marrow of the tibia was penetrated antegradely via the proximal anterior tibial metaphysis using a sterile bone marrow aspiration needle with a diameter of 3 mm. After reaching the marrow space and removing the trocar, the bone marrow was aspirated using a 2-ml syringe containing 0.1 ml heparin. The aspirated marrow was mixed in a 15-ml Falcon tube containing 5 ml of predigestion medium [0.5 ml of collagenase (1.5 mg/ml), 0.5 ml of hyaluronidase (1 mg/ml), and 4 ml of Verfaillie medium] [Reyes et al., 2001]. Then, the marrow aspirate was homogenized with a pipette. The aspirate was subsequently left to incubate at 39°C while spinning at 35 rpm continuously for 8 h (RM 540; CAT, Stauffen, Germany). Once digestion had ceased, 10 ml of phosphate-buffered saline (PBS) was added, and the predigested marrow aspirate was filtered using a 40-μm filter. The samples were washed in PBS (1:2) and centrifuged for 10 min at 677 *g*. Subsequently, the cells were counted and afterwards plated in cell culture flasks (Easy Flask filter, Nunclon™ surface; Nunc A/S, Roskilde, Denmark) in modified expansion medium according to Verfaillie with the addition of 2% fetal calf serum (FCS) [Reyes et al., 2001]. After 24 h, nonadhesive cells were discarded and adhesive cells were washed once with PBS. Standard culturing conditions were used (37°C, 5% CO_2), and the medium was changed twice a week. At 80–90% confluence, cells were harvested with trypsin/EDTA (Biochrom, Berlin, Germany) and replated by splitting usually 1:3 at a density of 50–60%. Cells were cultivated until passages 2–4, equaling 16–19 population doublings. The mesenchymal differentiation potential for the osteogenic, the chondrogenic, and the adipogenic lineages was demonstrated qualitatively in vitro from aliquots of the adherent cells of the bone marrow aspirate as reported previously [Vogel et al., 2006]. Therefore, the cells fulfill the criteria of mesenchymal stem/stromal cells [Reyes et al., 2001].

Plasmid Preparation and Transfection of Rabbit BMSC

Human VEGF (GeneBank accession No. XM 004512) was integrated into the pCR3.1 plasmid (Invitrogen, Karlsruhe, Germany) as published previously [Nikol et al., 2002; Geiger et al., 2005] using the EcoRI restriction site. This resulted in a 5.6-kb vector containing the human $VEGF_{165}$ cDNA fragment, creating the plasmid $phVEGF_{165}$. For large scale endotoxin-free plasmid DNA production of $phVEGF_{165}$ and pCR3.1, an EndoFree Plasmid Giga Kit (Qiagen, Hilden, Germany) was used according to the manufacturer's protocol. Rabbit BMSC were cultured in cell culture flasks as described above under standard conditions (37°C with 5% CO_2). For transfection, cells were seeded at 20×10^3 cells/cm^2 and allowed to adhere overnight. Transfection was performed with 1 μg of plasmid DNA of $phVEGF_{165}$ or empty pCR3.1 combined with 3 μl of metafectene per 100.000 cells in serum-free medium. After 6 h the medium was changed to BMSC culture medium and cells were kept overnight. Transfected cells (5×10^6) were then seeded on each scaffold.

Loading of Cells and Application of PRP

All ceramics were incubated overnight at 4°C in 40 μM/ml fibronectin (Sigma, Taufkirchen, Germany) solution diluted in PBS to improve the adhesion of the cells and because it was found to be beneficial for bone formation [Vogel et al., 2006]. The cells to be transplanted were detached from the culture flasks by trypsin and counted. Five million cells were then resuspended in 3 ml of culture medium and transferred into a 5-ml tube. The ceramics were placed into the medium containing the cells. After 1.5 h of continuous spinning at 37°C (35×/min) to achieve a homogeneous distribution of the cells on the surface of the scaffold, the ceramics were placed into a six-well plate. The medium containing the cells was centrifuged twice at 800 *g* for 5 min, and the resulting cell pellet was resuspended in 70 μl of culture medium and applied to the ceramics. Previous studies demonstrated that loading BMSC statically on CDHA had an efficiency of 95% [Kasten et al., 2005]. After loading of the cells, the BMSC remain in the superficial layers within a depth of 1–2 mm [Kasten et al., 2005]. As published previously, 40 ml of freshly thawed PRP was applied to the ceramics of the PRP group, and subsequently 10 μl of thrombin (0.8 IU activity)-calcium chloride (1 M) solution (1:1) (Tissucol-duo; Baxter, Unterschleissheim, Germany) was added directly before implantation [Kasten et al., 2008b]. Animals that received PRP had no local inflammatory response, and no systemic immune responses such as fevers were noticed [Kasten et al., 2008b].

Surgical Procedure

The animal model was adapted from Wittbjer et al. [1982] as described previously. Briefly, unilateral 15-mm critical-size defects were created in the distal radial diaphysis. The rabbits were anesthetized with an intramuscular injection of ketamine hydrochloride (50 mg/kg body weight, Hostaket®; Intervet, Tönisvorst, Germany) and xylazine (5 mg/kg body weight, Rompun®; Bayer Vital, Leverkusen, Germany). An antibiotic (netilmicin 4 mg/kg body weight, Certomycin®; Essex Pharma, Munich, Germany) was administered perioperatively. A superomedial incision of 3 cm was made over the distal radius, soft tissues were dissected, and the bone was exposed by gentle retraction of the muscles. A Hohmann retractor was placed between the ulna and radius to protect the ulna. A 15-mm segmental diaphyseal defect was created with an oscillating saw under irrigation with 0.9 vol% sterile saline solution. The periosteum was removed with the bone and 5 mm of periosteum was stripped from each side of the remaining proximal as well as distal main fragment. The defect was irrigated with sterile physiological saline solution, and the scaffold was press fitted into the defect. Muscles, fascia, and skin were separately closed over the defect with 4-0 resorbable sutures (Ethilon; Ethicon, Norderstedt, Germany). Fixation of the osteotomized radius was unnecessary because of the fibro-osseous union of ulna

and radius proximal and distal to the surgical site and the press fit of the implant. Although a certain micromotion of the implant might be possible due to resorption of the scaffold, no dislocation could be found in the subsequent control radiographs. Postoperatively, 4 mg/kg body weight of carprofen was given as needed for pain. There were no differences in carprofen administration among the groups. Water and food were supplied ad libitum. After 16 weeks the animals were euthanized. Samples were excised en bloc with the surrounding soft tissues and immediately placed in paraformaldehyde 4%.

Radiographic Evaluation

Standardized anterior-posterior and lateral radiographs were taken immediately postoperatively and every 4 weeks thereafter until sacrifice after week 16 to monitor the placement of the graft and the bony integration. An ultra-high-definition film (44 kV and 2.2 mA with a constant X-ray to object-to-film distance of 171 cm) was used. No dislocation of the scaffold was noticed in this time period.

Micro-Computer Tomography

Each specimen containing the 1.5-cm segmental defect and 0.5 cm of proximal and 0.5 cm of distal cortical bone adjacent to the defect was examined with a micro-computer tomography (μ-CT) system (Fanbeam Micro-CT; Stratec, Stuttgart, Germany). The microfocus of the X-ray source of the μ-CT system had a spot size of 7 μm and a maximum voltage of 36 kV. The image matrix was 1,024 × 1,024 pixels. The specimens were placed in a sample holder filled with water. They were oriented in such a way that the long axis of the block was parallel to the axis of the sample holder. A high-resolution protocol (slice thickness 120 μm, feed 60 μm, and pixel size 60 μm) was applied. Depending on the length of the specimens, up to 180 slices were scanned perpendicular to the block. To determine the amount of newly formed bone tissue, the best threshold for the CDHA scaffold alone was selected visually followed by determination of the threshold for the CDHA scaffold and newly formed bone together. Furthermore, an empty cylinder of the scaffold and several bones were scanned prior to our investigation for comparison. In addition, the ranges and means of the gray levels characteristic of the CDHA scaffold and newly formed bone were determined. The CDHA scaffold showed a mean gray level of 160 ± 15, while that of the newly formed bone was 60 ± 15. The visually determined threshold to separate the CDHA scaffold from newly formed bone was set at 100, allowing reliable distinction between the two tissue types. Finally, μ-CT slices were compared with the corresponding histological slides to verify the reliability of the discrimination criteria. The digitized data were analyzed with VG Studio Max 1.2.1 software (Volume Graphics, Heidelberg, Germany), and the amount of new bone formation (newly formed bone voxels per complete tissue voxels of the initially implanted CDHA volume) was calculated. Resorption was calculated by dividing the voxels of the ceramic that was present after 16 weeks by the voxels of the mean of three CDHA cylinders that were not implanted.

Histology and Immunohistochemical Staining for Blood Vessels

After μ-CT analysis, the nondecalcified specimens were dehydrated in ascending grades of alcohol and embedded in Technovit (Technovit 7200 VLC; Kulzer GmbH, Wehrheim, Germany). During embedding, the positioning of the radius was standardized in an attempt to ensure that the same region was evaluated in all specimens. Then, 50-μm coronal sections with the radius and ulna parallel were made using a sawing and grinding technique (Exakt Apparatebau, Hamburg, Germany). One section of each sample was stained with Giemsa and toluidine-blue (Waldeck GmbH & Co., Division Chroma, Münster, Germany) and three were used for immunohistological staining of the vessels. The sections were examined using a light microscope (Axioplan 2 Imaging; Zeiss, Göttingen, Germany). The Giemsa/toluidine-stained specimens were digitized and analyzed with the program Image J (National Institutes of Health) [Abramoff et al., 2004]. The type of tissue was identified manually, marked, and assigned to a color. In detail, the areas of newly formed bone, connective tissue, and ceramic were calculated per total bone defect area.

Endothelial cells were stained with a monoclonal mouse anti-human CD-31 antibody (Clone: JC70A; DakoCytomation, Glastrup, Denmark; dilution 1:20) as dexcribed previously [Geiger et al., 2007b]. The sections were deacrylated in two steps with 2-methoxy ethyl acetate for 8h, incubated 3 times with XEM for 30 min, and rehydrated followed by digestion with 0.1% chymotrypsin (Sigma-Aldrich, Deisenhofen, Germany; 60 min, 37°C). Endogenous peroxidase was blocked by 3% hydrogen peroxide for 30 min and nonspecific background was blocked using 5% BSA/PBS (30 min). Because the CD-31 antibody is specific for endothelial cells, vessels were stained with a monoclonal mouse anti-human CD-31 antibody (Clone: JC70A; DakoCytomation; dilution 1:20) overnight at 4°C. Primary antibody was detected with the CSA biotin-free tyramide signal amplification system (DakoCytomation) according to the manufacturer's instructions. Incubation with secondary antibody, anti-mouse-immunoglobulin-HRP, amplification reagent, and anti-fluorescein-HRP lasted 30 min each and incubation with DAB chromogen took 15 min. Counterstaining was avoided due to possible influencing of the computer-based image evaluation.

On each slide, six standardized regions of interest with an area of 0.6 mm^2 were photographed at a ×10 magnification with the Axioplan 2 (Carl-Zeiss, Oberkochen, Germany). Slices were randomly selected before staining by a blinded investigator, and blood vessels were marked by two independent examiners blinded for groups and treatment. The number of vessels in each region of interest was determined with the help of the Axiovision 4.4 program (Carl-Zeiss). The mean values of the two observers for each parameter were calculated.

Statistics

Data analysis was performed with SPSS for Windows 15.0 (SPSS, Inc., Chicago, Ill., USA). Mean values and standard deviations were calculated. The main outcome measures were newly formed bone and ceramic resorption in μ-CT and vessel formation in histology. These were examined by multifactorial analysis of variance (ANOVA). Differences between the independent variables were checked in post hoc tests [Tukey's studentized range (HSD) tests for variables]. The alpha error was consequently adjusted. $p < 0.05$ was considered statistically significant. All tests were two-tailed.

Table 1. New bone formation in μ-CT

Independent variable	Subgroup	Mean value ± SD (% of total CDHA cylinder volume)	n	Post hoc comparison*	p value†/ d.f./z value
Bone formation in μ-CT	CDHA + VEGF transfected BMSC	11 ± 3.6	6	a	0.0001/4/13.86
	CDHA + rabbit BMSC	22.83 ± 5.98	6	b	
	CDHA + PRP	24.8 ± 5.54	5	b	
	CDHA + rabbit BMSC + PRP	26.67 ± 6.28	6	b	
	CDHA only	11 ± 3.58	6	a	

* Different letters indicates significant differences between homogeneous subgroups at an alpha level of $p < 0.05$. For example, the VEGF group (post hoc comparison, letter a) is significantly different from CDHA + rabbit BMSC (letter b) but not from the CDHA only group (letter a).
† By ANOVA.

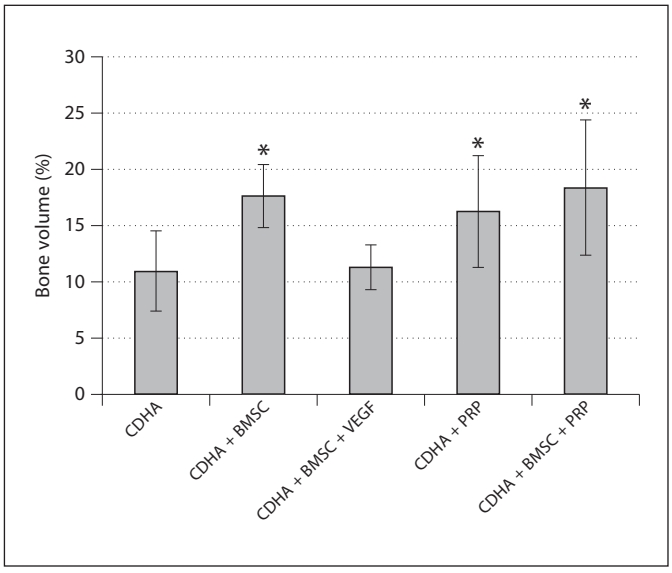

Fig. 1. There was a significantly higher ($p < 0.05$) bone formation measured in μ-CT in the PRP group and the BMSC + PRP group as well as in the BMSC group compared to the control CDHA group without cells and the VEGF group. Asterisks indicate significantly higher values compared to the CDHA and VEGF group.

Results

Bone Formation in μ-CT and Histology

Transfection of the BMSC with VEGF did not lead to a significant increase in bone formation as compared to CDHA controls (fig. 1; table 1). This was in contrast to the groups with PRP and BMSC that showed significantly higher ($p < 0.05$) bone formation than the control CDHA group (fig. 1). In detail μ-CT analysis showed higher bone formation in the PRP group, with 24.8% of total CDHA cylinder volume (SD 5.5), and in the BMSC + PRP group (26.7%, SD 6.3), as well as in the BMSC group (22.8%, SD 6), compared to the control CDHA group without cells (11%, SD 3.6) and the VEGF group (11.3%, SD 2) ($p < 0.05$). Analysis of the histology specimen showed that novel bone formation was mainly at the edges of the scaffold that were in close contact with the osteotomy surface of the radius (fig. 2). Obviously, the environment in this area is most favorable for bone formation due to direct cell contact and invasion from the adjacent bone. However, there was also bone formation within the pores of the scaffold (fig. 2a). Higher magnification images were able to demonstrate direct osteoblast formation on the CDHA scaffold (fig. 2b). In histology, there were no inflammatory reactions like macrophages or lymphocyte aggregations visible due to biodegradation of the scaffold.

Biodegradation of the CDHA Scaffold

Biodegradation of the scaffold was increased over the course of 16 weeks in all groups compared to the CHDA control ($p < 0.05$). In the VEGF group the remaining ceramic/total ceramic volume was 64.8% (SD 3.5), in the PRP group it was 57% (SD 7.2), in the PRP + BMSC group it was 60.2% (SD 7.9), and in the CDHA + BMSC group it was 61.8% (SD 5.8). The empty CDHA control had less biodegradation (75%, SD 8).

Vascularization in Histology

VEGF transfection of the BMSC led to higher vascularization of the scaffolds than in the BMSC and PRP

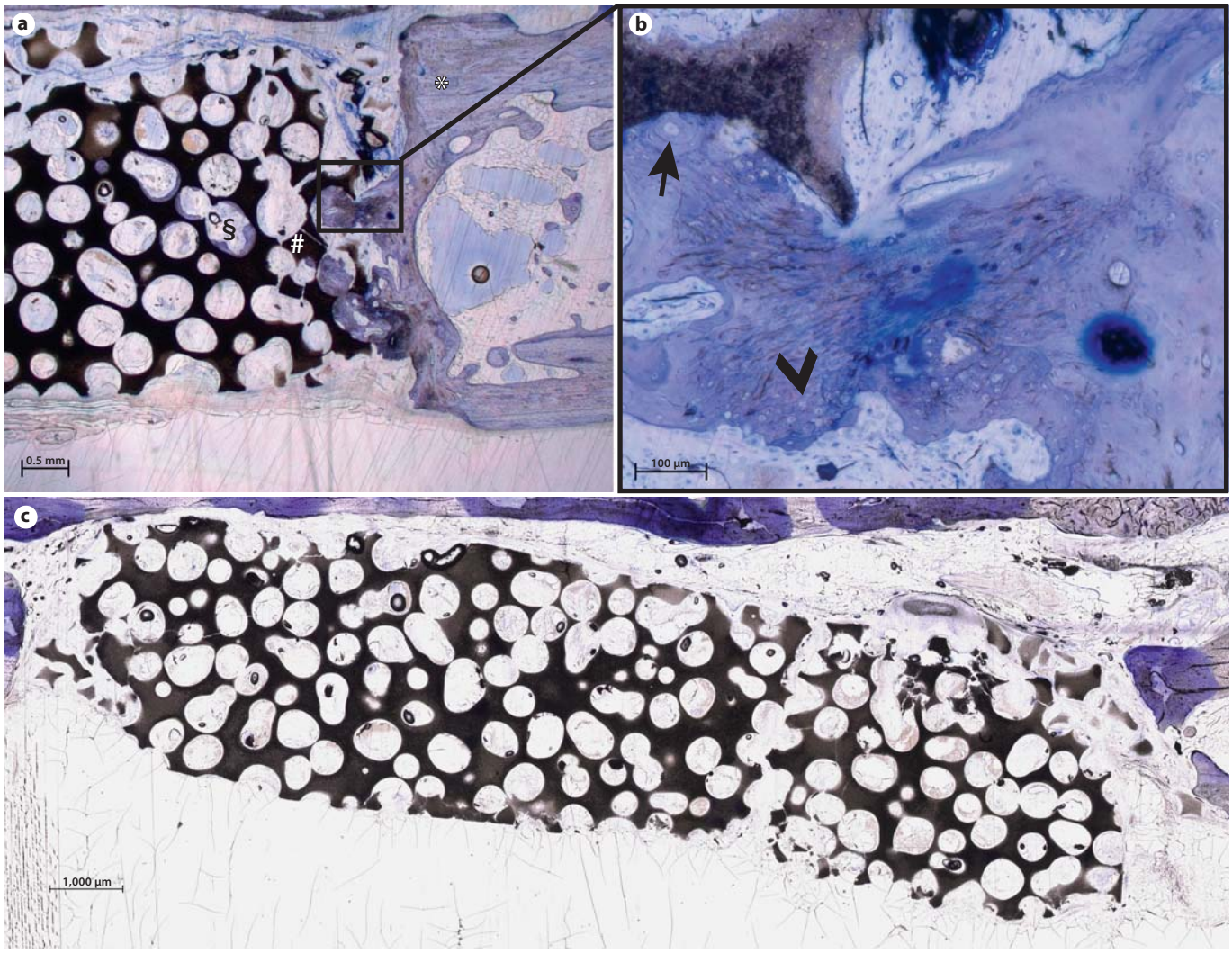

Fig. 2. This histology specimen (toluidine blue staining) from the VEGF group demonstrates bone formation at the edges of the CDHA scaffold (#) in close contact with the remaining native bone (*) (**a**). The lower magnification (**a**) reveals bone formation within the pores of the scaffold (§). The higher magnification shows the direct contact of the novel bone with the scaffold (arrow) and osteoblasts (arrowhead) (**b**). **c** The figure shows the control of an empty CDHA scaffold that is not integrated into the bone and does not show any bony ingrowth.

groups ($p < 0.05$), but the result was similar to that of the CDHA + PRP + BMSC group (fig. 3). The VEGF group had 21.31 vessels/mm^2 (SD 3.2) and the BMC + PRP group had 20.57 vessels/mm^2 (SD 6.71) compared to 13.06 vessels/mm^2 (SD 0.93) in the CDHA control, 15.39 (SD 2.39) vessels/mm^2 in the BMSC group, and 16.02 vessels/mm^2 (SD 6.71) in the PRP group (fig. 3). Staining for CD-31 displayed the vessels within the scaffold even in deeper areas of the biomaterial (fig. 4a, b).

Discussion

The hypothesis of this study was that the osteogenic capacity of VEGF-transfected BMSC on a ceramic scaffold in a critical-size long bone defect is equal to the addition of PRP and BMSC. A critical-size defect in this context means that the defect cannot heal on its own in contrast to, for example, fractures. Our data demonstrates that VEGF-transfected BMSC and the combination of PRP and BMSC are equally effective in improving vascu-

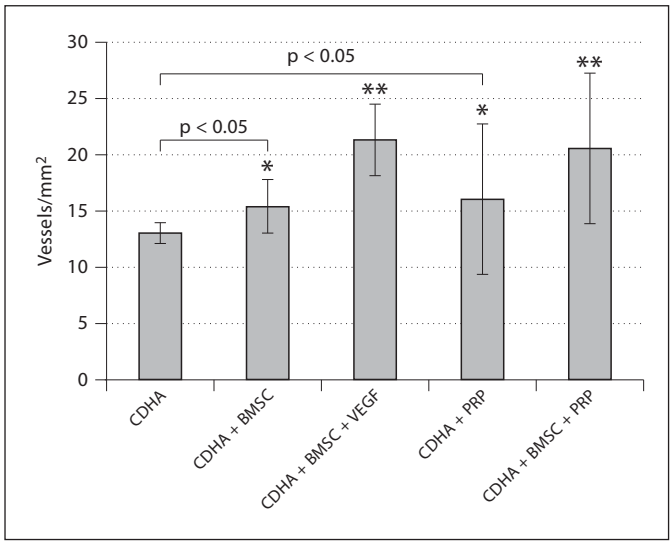

Fig. 3. VEGF transfection promoted vascularization of the scaffolds significantly in contrast to BMSC and PRP ($p < 0.05$) but was similar to the CDHA + PRP + BMSC group. * Indicates significant differences to the empty CDHA control; ** indicates that the VEGF and PRP + BMSC groups had higher numbers of vessels than the control CDHA, the BMSC group, and the PRP group.

Fig. 4. a CD-31 staining allowed counting of the vessels within the specimen from the VEGF group. The higher magnification image shows a cut through a vessel (*) with staining of the endothelial cells (**b**).

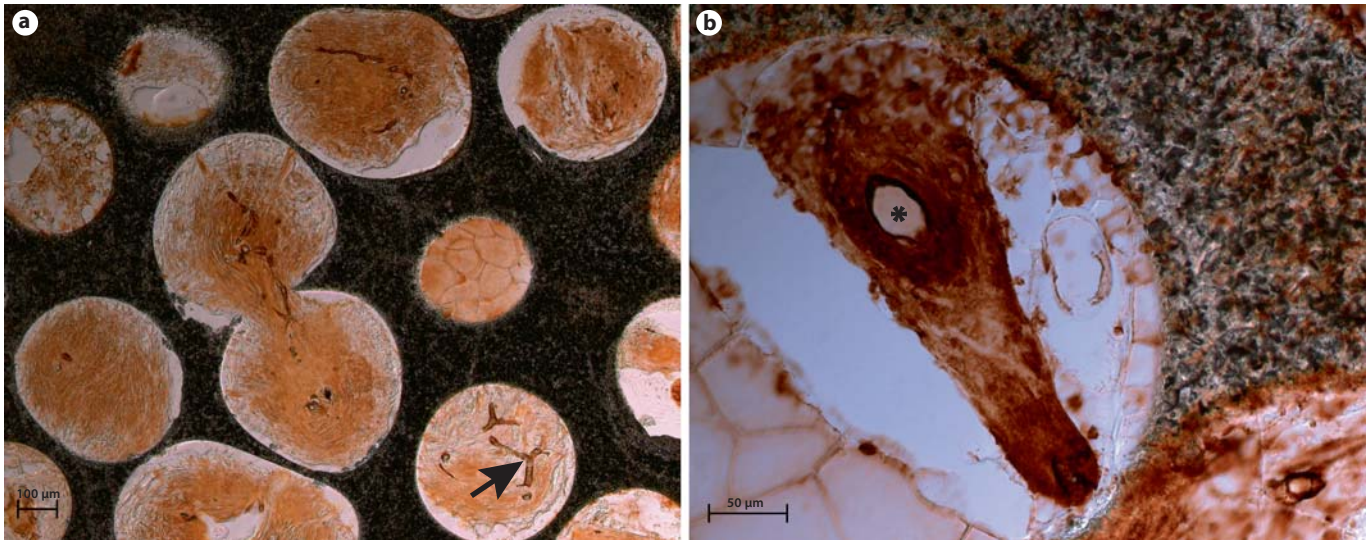

larization, but bony healing was better in the combination of BMSC and PRP than with VEGF-transfected BMSC.

In general, the concept of tissue engineering is based on a combination of stem cells, biomaterials, and growth factors. In the current study the same high surface scaffold CDHA was used to warrant comparison of the results. CDHA was chosen because it had shown favorable results in bone tissue engineering in the past [Kasten et al., 2005; Kasten et al., 2006; Kasten et al., 2008b]. Furthermore, bone marrow-derived stem cells (BMSC) have been shown to improve bone regeneration in comparison to the use of biomaterials alone. Consequently, the biomaterial and BMSC was determined to be the control for this study.

A critical issue in bone regeneration is a sufficient vascular supply as implantation of large bone grafts without adequate vascularity results in apoptosis and cartilage formation [Muschler et al., 2004]. This is supported by the fact that bone repair has been shown to benefit from increased angiogenesis [Santos and Reis, 2010]. The main focus of this study was to compare the effect of two ways to improve vascularization and subsequently bone regeneration. Firstly, VEGF-transfected BMSC and, secondly, a mix of growth factors derived from platelets (PRP) were used.

The growth factor VEGF has the potential to promote differentiation of common progenitor cells to angiogenic and osteogenic lineages. In embryonic development,

VEGFA has been considered of great importance for vascularization and patterning of the bone growth plate [Gerber et al., 1999]. VEGFA has been shown to increase bone formation in long bone defect models [Street et al., 2002; Geiger et al., 2005], promote osteoblast differentiation in an autocrine fashion [Street et al., 2002], inhibit osteoblast apoptosis [Street and Lenehan, 2009], and induce endothelial cells from human embryonic stem cells [Nourse et al., 2010]. Recently, it was shown that local application of VEGFA to human adipose-derived stem cells significantly improved the healing of critical-size calvarial defects in vivo and gene activated matrices (by VEGF) improved the healing of long bone defects in rabbits [Geiger et al., 2005]. This repair was accompanied by an enhancement of angiogenesis [Behr et al., 2011]. Orchestration of bone formation is inevitably linked to a cross talk between osteoblasts and endothelial cells [Brandi and Collin-Osdoby, 2006]. An important mediator of angiogenesis is VEGFA [Keramaris et al., 2008], which is physiologically released during fracture healing [Street et al., 2000]. A study demonstrated that VEGFA is primarily released by osteoblasts, whereas its action is conducted through endothelial cells [Clarkin et al., 2008]. Osteogenic effects of VEGFA on osteoblasts, such as increased bone nodule formation and alkaline phosphatase activity, have been reported in vitro [Street et al., 2002]. Moreover, VEGFA increased bone healing in vivo, whereupon delivery of VEGFA was performed with bioresorbable polylactic acid depot scaffolds or gene-activated matrices [Street et al., 2002; Geiger et al., 2005].

We are aware that the effect of a growth factor like VEGF is highly dependent on the method of administration, dosage, and other circumstances. This is why other authors found conflicting results on the effect of VEGF [Peng et al., 2002; Tarkka et al., 2003]. Our group has used different methods of administration in previous studies [Geiger et al., 2005, 2007b]. The way we used VEGF in this study has proven to be effective before [Geiger et al., 2007b]. As we wanted to focus on the different effects of VEGF and PRP, we did not change the experimental setting. Examination of other ways to use VEGF remains an interesting topic for future studies.

Another popular way of improving vascularization, and subsequently bone formation, is PRP. In 1998, Marx et al. [1998] reported their initial results of PRP as a source of autogenous thrombocytic growth factors for the reconstruction of maxillofacial defects in humans. They found that PRP resulted in quicker maturation of autogenous bone transplants and higher bone density [Marx et al., 1998]. From basic science, we know that overall platelets promote bone healing mainly by mitogenic effects, whereas the direct osteogenic effects are less pronounced [Kasten et al., 2008a]. The growth factors (PDGF, TGF, IGF, etc.) of the platelets are released after degranulation and act through a variety of pathways: the principal actions of PDGF are chemotaxis, mitogenesis, and angiogenesis and start the bone healing cascade. The PDGF effect is exerted via receptors that have tyrosine kinase activity. IL-1, TNF-α, and TGF-β_1 affect the binding of PDGF [Solheim, 1998]. TGF-β_1 is not only released by platelets but also synthesized by osteoblasts and chondrocytes throughout the healing process. TGF-β activates the transformation of osteoprogenitor cells into osteoblasts, which in turn initiate the production of extracellular matrix, or soft callus [Lieberman et al., 2002]. IGF-I promotes bone matrix formation (type I collagen and noncollagenous matrix proteins) by fully differentiated osteoblasts [Canalis, 1980] and is more potent than IGF-II [Lieberman et al., 2002]. IGF-II acts at a later stage of endochondral bone formation and stimulates type I collagen production, cartilage matrix synthesis, and cellular proliferation [Prisell et al., 1993].

Besides the growth factors mentioned above, fibrin, fibronectin, and vitronectin play an important role as cell adhesions molecules. Fibronectin and vitronectin seem to be able to provide a foothold for cells as they move [Clark et al., 1982; Clark et al., 1996]. Fibrin is a cross-linked protein derived from the fibrinogen in plasma. Like fibronectin and vitronectin, it contributes to cell movement in the wound. When fibrin cross-linking occurs as part of the clotting process, it traps platelets and provides a scaffold or surface for cell movement.

Recently there have been conflicting reports about the effect of PRP plasma, and there is no consensus regarding the role of PRP in bone regeneration: there are multiple favorable results of PRP regarding the improvement of proliferation of MSC in vitro and in vivo after ectopic implantation, but also in animal models with critical-size bone defects [Kasten et al., 2008b; Bi et al., 2010; Hakimi et al., 2010; Hartmann et al., 2010; Jungbluth et al., 2010; Niemeyer et al., 2010; Bae et al., 2011; Liu et al., 2011]. However, there is also a relevant number of studies reporting no or minimal effects of PRP on bone formation [Li et al., 2004; Roldan et al., 2004; Plachokova et al., 2007; Thor et al., 2007; Vasconcelos Gurgel et al., 2007; You et al., 2007; Miloro et al., 2010; Kazakos et al., 2011]. Regarding its clinical use in maxillofacial surgery, a recent meta-analysis indicated that there was sufficient evidence to support the use of PRP for bone formation on a sinus bone graft, whereas there was no significant effect on the

implant survival and bone-to-implant contact [Bae et al., 2011]. In orthopedic surgery, some authors report positive outcomes in leg lengthening procedures and spinal fusions [Bi et al., 2010; Hartmann et al., 2010]. In summary, the role of PRP remains controversial. Several studies have shown a positive effect, mainly on early bone healing, while others have not. However, most studies can hardly be compared because the study designs were very different. Factors that can influence the efficacy of PRP as a promoter of bone healing are: (1) the biomaterial, (2) the species, (3) the site of implantation, and (4) the preparation and activation of the PRP.

Rabbit thrombocytes have a survival time of 2–6 days and the growth factors are present for 1–2 days after degranulation. The platelet count in NZWR ranges from 282 × 103/mm^3 to 1,067 × 103/mm^3, with an average of 563 × 103/mm^3 in 100 normal rabbits [EBBE et al., 1965; Mitruka and Rawnley, 1977]

A key question in the interpretation of this study is why bone formation of VEGF-transfected cells was inferior to the use of PRP. There are some possible explanations for this finding. Although the selective increase of the single growth factor VEGF increased vascularization in histology, this did not translate into sufficient bone formation. This can be explained by the fact that bone healing relies on a 'symphony' of different growth factors that are secreted at different time points [Street et al., 2000]. The mixture of growth factors of PRP obviously mimics nature better than a single growth factor, which might resulted in stronger bone formation after application of PRP. Another explanation could be that plasmid transfection alters the BMSC in a way that reduces bone formation. Maybe the transfection inhibits transcription programs that are necessary for proper functioning and differentiation of the BMSC in bone healing. Similar phenomena were reported after transfection of BMSC with growth differentiation factor-5 (GDF-5) for tendon regeneration [Rickert et al., 2005].

Conclusion

Expression of VEGF in BMSC as a single growth factor does not seem to be as effective as expanded BMSC alone or PRP for healing of a critical-size long bone defect in rabbits. The mixture of growth factors in PRP seems to be more useful for bone formation than the overexpression of a single growth factor that mainly increases vascularization.

Acknowledgements

The work was performed at the Department of Orthopaedic Surgery of the University of Heidelberg, Germany.

The authors wish to thank Prof. W. Richter and the Division of Experimental Orthopaedics for general support and especially Regina Foehr and Katrin Goetzke for her excellent technical assistance in preparing the histology.

We further thank Dipl.-Ing. Dirk Bormann of the Institut für Werkstoffkunde Leibniz Universität Hannover, and Krisztian Szalay from the Semmelweis University in Budapest, for assistance with the μ-CT.

This work was supported by a grant from the research fund of the Stiftung Orthopaedische Universitätsklinik Heidelberg.

We also thank Dr. Reto Luginbühl from the Dr. h.c. Robert Mathys Foundation for providing the scaffolds.

References

Abramoff, M.D., P.J. Magelhaes, S.J. Ram (2004) Image processing with Image J. Biophotonics Int *11:* 36–42.

Arrington, E.D., W.J. Smith, H.G. Chambers, A.L. Bucknell, N.A. Davino (1996) Complications of iliac crest bone graft harvesting. Clin Orthop *329:* 300–309.

Bae, J.H., Y.K. Kim, S.K. Myung (2011) Effects of platelet-rich plasma on sinus bone graft: meta-analysis. J Periodontol *82:* 660–667.

Behr, B., C. Tang, G. Germann, M.T. Longaker, N. Quarto (2011) Locally applied vascular endothelial growth factor a increases the osteogenic healing capacity of human adipose-derived stem cells by promoting osteogenic and endothelial differentiation. Stem Cells *29:* 286–296.

Bi, L., W. Cheng, H. Fan, G. Pei (2010) Reconstruction of goat tibial defects using an injectable tricalcium phosphate/chitosan in combination with autologous platelet-rich plasma. Biomaterials *31:* 3201–3211.

Bohner, M. (2000) Calcium orthophosphates in medicine: from ceramics to calcium phosphate cements. Injury *31(suppl 4):* 37–47.

Brandi, M.L., P. Collin-Osdoby (2006) Vascular biology and the skeleton. J Bone Miner Res *21:* 183–192.

Bruder S.P., D.J. Fink, A.I. Caplan (1994) Mesenchymal stem cells in bone development, bone repair, and skeletal regeneration therapy. J Cell Biochem *56:* 283–294.

Burchardt, H., W.F. Enneking (1978) Transplantation of bone. Surg Clin North Am *58:* 403–427.

Canalis, E. (1980) Effect of insulinlike growth factor I on DNA and protein synthesis in cultured rat calvaria. J Clin Invest *66:* 709–719.

Clark, R.A., P. DellaPelle, E. Manseau, J.M. Lanigan, H.F. Dvorak, R.B. Colvin (1982) Blood vessel fibronectin increases in conjunction with endothelial cell proliferation and capillary ingrowth during wound healing. J Invest Dermatol *79:* 269–276.

Clark, R.A., M.G. Tonnesen, J. Gailit, D.A. Cheresh (1996) Transient functional expression of alphaVbeta 3 on vascular cells during wound repair. Am J Pathol *148:* 1407–1421.

Clarkin, C.E., R.J. Emery, A.A. Pitsillides, C.P. Wheeler-Jones (2008) Evaluation of VEGF-mediated signaling in primary human cells reveals a paracrine action for VEGF in osteoblast-mediated crosstalk to endothelial cells. J Cell Physiol *214:* 537–544.

Damien, C, R. Parsons (1991) Bone graft and bone graft substitutes: review of current technology and applications. J Appl Biomater *2:* 187–208.

DePalma, A.F., R.H. Rothman, G.E. Lewinnek, S.T. Canale (1972) Anterior interbody fusion for severe cervical disc degeneration. Surg Gynecol Obstet *134:* 755–758.

Ebbe, S., M. Baldini, J. Donovan (1965) Comparative studies of platelet survival by different methods in the rabbit. Blood *25:* 548–566.

Geiger, F., H. Bertram, I. Berger, H. Lorenz, O. Wall, C. Eckhardt, H.G. Simank, W. Richter (2005) Vascular endothelial growth factor gene-activated matrix (VEGF165-GAM) enhances osteogenesis and angiogenesis in large segmental bone defects. J Bone Miner Res *20:* 2028–2035.

Geiger, F., H. Lorenz, W. Xu, K. Szalay, P. Kasten, L. Claes, P. Augat, W. Richter (2007a) VEGF producing bone marrow stromal cells (BMSC) enhance vascularization and resorption of a natural coral bone substitute. Bone *41:* 516–522.

Geiger, F., H. Lorenz, W. Xu, K. Szalay, P. Kasten, L. Claes, P. Augat, W. Richter (2007b) VEGF producing bone marrow stromal cells (BMSC) enhance vascularization and resorption of a natural coral bone substitute. Bone *41:* 516–522.

Gerber, H.P., T.H. Vu, A.M. Ryan, J. Kowalski, Z. Werb, N. Ferrara (1999) VEGF couples hypertrophic cartilage remodeling, ossification and angiogenesis during endochondral bone formation. Nat Med *5:* 623–628.

Hakimi, M., P. Jungbluth, M. Sager, M. Betsch, M. Herten, J. Becker, J. Windolf, M. Wild (2010) Combined use of platelet-rich plasma and autologous bone grafts in the treatment of long bone defects in mini-pigs. Injury *41:* 717–723.

Hartmann, E.K., T. Heintel, R.H. Morrison, A. Weckbach (2010) Influence of platelet-rich plasma on the anterior fusion in spinal injuries: a qualitative and quantitative analysis using computer tomography. Arch Orthop Trauma Surg *130:* 909–914.

Janicki, P., P. Kasten, K. Kleinschmidt, R. Luginbuehl, W. Richter (2010) Chondrogenic preinduction of human mesenchymal stem cells on beta-TCP: enhanced bone quality by endochondral heterotopic bone formation. Acta Biomater *6:* 3292–3301.

Jungbluth, P., M. Wild, J.P. Grassmann, E. Ar, M. Sager, M. Herten, M. Jager, J. Becker, J. Windolf, M. Hakimi (2010) Platelet-rich plasma on calcium phosphate granules promotes metaphyseal bone healing in mini-pigs. J Orthop Res *28:* 1448–1455.

Kasten, P., I. Beyen, D. Bormann, R. Luginbuhl, F. Ploger, W. Richter (2010) The effect of two point mutations in GDF-5 on ectopic bone formation in a beta-tricalciumphosphate scaffold. Biomaterials *31:* 3878–3884.

Kasten, P., R. Luginbuhl, M. van Griensven, T. Barkhausen, C. Krettek, M. Bohner, U. Bosch (2003) Comparison of human bone marrow stromal cells seeded on calcium-deficient hydroxyapatite, beta-tricalcium phosphate and demineralized bone matrix. Biomaterials *24:* 2593–2603.

Kasten, P., J. Vogel, I. Beyen, S. Weiss, P. Niemeyer, A. Leo, R. Luginbuhl (2008a) Effect of platelet-rich plasma on the in vitro proliferation and osteogenic differentiation of human mesenchymal stem cells on distinct calcium phosphate scaffolds: the specific surface area makes a difference. J Biomater Appl *23:* 169–188.

Kasten, P., J. Vogel, F. Geiger, P. Niemeyer, R. Luginbuhl, K. Szalay (2008b) The effect of platelet-rich plasma on healing in critical-size long-bone defects. Biomaterials *29:* 3983–3992.

Kasten, P., J. Vogel, R. Luginbuhl, P. Niemeyer, M. Tonak, H. Lorenz, L. Helbig, S. Weiss, J. Fellenberg, A. Leo, H.G. Simank, W. Richter (2005) Ectopic bone formation associated with mesenchymal stem cells in a resorbable calcium deficient hydroxyapatite carrier. Biomaterials *26:* 5879–5889.

Kasten, P., J. Vogel, R. Luginbuhl, P. Niemeyer, S. Weiss, S. Schneider, M. Kramer, A. Leo, W. Richter (2006) Influence of platelet-rich plasma on osteogenic differentiation of mesenchymal stem cells and ectopic bone formation in calcium phosphate ceramics. Cells Tissues Organs *183:* 68–79.

Kazakos, K., D.N. Lyras, V. Thomaidis, G. Agrogiannis, S. Botaitis, G. Drosos, A. Kokka, D. Verettas (2011) Application of PRP gel alone or in combination with guided bone regeneration does not enhance bone healing process: an experimental study in rabbits. J Craniomaxillofac Surg *39:* 49–53.

Keramaris, N.C., G.M. Calori, V.S. Nikolaou, E.H. Schemitsch, P.V. Giannoudis (2008) Fracture vascularity and bone healing: a systematic review of the role of VEGF. Injury *39(suppl 2):* S45–S57.

Kiuru, J., L. Viinikka, G. Myllyla, K. Personen, J. Perheentupa (1991) Cytoskeleton-dependent release of human platelet epidermal growth factor. Life Sci *49:* 1997–2003.

Laurencin, C.T., A.M. Ambrosio, M.D. Borden, J.A. Cooper Jr. (1999) Tissue engineering: orthopedic applications. Annu Rev Biomed Eng *1:* 19–46.

LeGeros, R.Z. (2002) Properties of osteoconductive biomaterials: calcium phosphates. Clin Orthop *395:* 81–98.

Li, H., X. Zou, Q. Xue, N. Egund, M. Lind, C. Bunger (2004) Anterior lumbar interbody fusion with carbon fiber cage loaded with bioceramics and platelet-rich plasma: an experimental study on pigs. Eur Spine J *13:* 354–358.

Lieberman, J.R., A. Daluiski, T.A. Einhorn (2002) The role of growth factors in the repair of bone: biology and clinical applications. J Bone Joint Surg Am *84-A:* 1032–1044.

Liu, H.Y., A.T. Wu, C.Y. Tsai, K.R. Chou, R. Zeng, M.F. Wang, W.C. Chang, S.M. Hwang, C.H. Su, W.P. Deng (2011) The balance between adipogenesis and osteogenesis in bone regeneration by platelet-rich plasma for age-related osteoporosis. Biomaterials *32:* 6773–6780.

Louisia, S., M. Stromboni, A. Meunier, L. Sedel, H. Petite (1999) Coral grafting supplemented with bone marrow. J Bone Joint Surg Br *81:* 719–724.

Marcacci, M., E. Kon, S. Zaffagnini, R. Giardino, M. Rocca, A. Corsi, A. Benvenuti, P. Bianco, R. Quarto, I. Martin, A. Muraglia, R. Cancedda (1999) Reconstruction of extensive long-bone defects in sheep using porous hydroxyapatite sponges. Calcif Tissue Int *64:* 83–90.

Marx, R.E., E.R. Carlson, R.M. Eichstaedt, S.R. Schimmele, J.E. Strauss, K.R. Georgeff, (1998) Platelet-rich plasma: Growth factor enhancement for bone grafts. Oral Surg Oral Med Oral Pathol Oral Radiol Endod *85:* 638–646.

Miloro, M., D.J. Haralson, V. Desa (2010) Bone healing in a rabbit mandibular defect using platelet-rich plasma. J Oral Maxillofac Surg *68:* 1225–1230.

Mitruka, B.M., H.M. Rawnley (1977) Clinical, Biochemical and Haematological Reference Values in Normal and Experimental Animals. New York, Masson Publishing USA, pp 134–135.

Muschler, G.F., C. Nakamoto, L.G. Griffith (2004) Engineering principles of clinical cell-based tissue engineering. J Bone Joint Surg Am *86-A:* 1541–1558.

Niemeyer, P., K. Fechner, S. Milz, W. Richter, N.P. Suedkamp, A.T. Mehlhorn, S. Pearce, P. Kasten (2010) Comparison of mesenchymal stem cells from bone marrow and adipose tissue for bone regeneration in a critical size defect of the sheep tibia and the influence of platelet-rich plasma. Biomaterials *31:* 3572–3579.

Niemeyer P., T.S. Schonberger, J. Hahn, P. Kasten, J. Fellenberg, N. Suedkamp, A.T. Mehlhorn, S. Milz, S. Pearce (2009a) Xenogenic transplantation of human mesenchymal stem cells in a critical size defect of the sheep tibia for bone regeneration. Tissue Eng Part A *16:* 33–43.

Niemeyer, P., K. Szalay, R. Luginbuhl, N.P. Sudkamp, P. Kasten (2009b) Transplantation of human mesenchymal stem cells in a non-autogenous setting for bone regeneration in a rabbit critical-size defect model. Acta Biomater *6:* 900–908.

Nikol, S., M.G. Engelmann, J. Pelisek, A. Fuchs, A. Golda, M. Shimizu, C. Mekkaoui, P.H. Rolland (2002) Local perivascular application of low amounts of a plasmid encoding for vascular endothelial growth factor (VEGF165) is efficient for therapeutic angiogenesis in pigs. Acta Physiol Scand *176:* 151–159.

Nourse, M.B., D.E. Halpin, M. Scatena, D.J. Mortisen, N.L. Tulloch, K.D. Hauch, B. Torok-Storb, B.D. Ratner, L. Pabon, C.E. Murry (2010) VEGF induces differentiation of functional endothelium from human embryonic stem cells: implications for tissue engineering. Arterioscler Thromb Vasc Biol *30:* 80–89.

Peng, H., V. Wright, A. Usas, B. Gearhart, H.C. Shen, J. Cummins, J. Huard (2002) Synergistic enhancement of bone formation and healing by stem cell-expressed VEGF and bone morphogenetic protein-4. J Clin Invest *110:* 751–759.

Plachokova, A.S., D.J. van den, P.J. Stoelinga, J.A. Jansen (2007) Early effect of platelet-rich plasma on bone healing in combination with an osteoconductive material in rat cranial defects. Clin Oral Implants Res *18:* 244–251.

Prisell, P.T., D. Edwall, J.B. Lindblad, A. Levinovitz, G. Norstedt (1993) Expression of insulin-like growth factors during bone induction in rat. Calcif Tissue Int *53:* 201–205.

Puelacher, W.C., J.P. Vacanti, N.F. Ferraro, B. Schloo, C.A. Vacanti (1996) Femoral shaft reconstruction using tissue-engineered growth of bone. Int J Oral Maxillofac Surg *25:* 223–228.

Reyes, M., T. Lund, T. Lenvik, D. Aguiar, L. Koodie, C.M. Verfaillie (2001) Purification and ex vivo expansion of postnatal human marrow mesodermal progenitor cells. Blood *98:* 2615–2625.

Rickert, M., H. Wang, P. Wieloch, H. Lorenz, E. Steck, D. Sabo, W. Richter (2005) Adenovirus-mediated gene transfer of growth and differentiation factor-5 into tenocytes and the healing rat Achilles tendon. Connect Tissue Res *46:* 175–183.

Roldan, J.C., S. Jepsen, J. Miller, S. Freitag, D.C. Rueger, Y. Acil, H. Terheyden (2004) Bone formation in the presence of platelet-rich plasma vs. bone morphogenetic protein-7. Bone *34:* 80–90.

Santos, M.I., R.L. Reis (2010) Vascularization in bone tissue engineering: physiology, current strategies, major hurdles and future challenges. Macromol Biosci *10:* 12–27.

Solheim, E. (1998) Growth factors in bone. Int Orthop *22:* 410–416.

Street, J., M. Bao, L. deGuzman, S. Bunting, F.V. Peale, Jr., N. Ferrara, H. Steinmetz, J. Hoeffel, J.L. Cleland, A. Daugherty, N. van Bruggen, H.P. Redmond, R.A. Carano, E.H. Filvaroff (2002) Vascular endothelial growth factor stimulates bone repair by promoting angiogenesis and bone turnover. Proc Natl Acad Sci USA *99:* 9656–9661.

Street, J., B. Lenehan (2009) Vascular endothelial growth factor regulates osteoblast survival – evidence for an autocrine feedback mechanism. J Orthop Surg Res *4:* 19.

Street, J., D. Winter, J.H. Wang, A. Wakai, A. McGuinness, H.P. Redmond (2000) Is human fracture hematoma inherently angiogenic? Clin Orthop Relat Res *378:* 224–237.

Tarkka, T., A. Sipola, T. Jamsa, Y. Soini, S. Yla-Herttuala, J. Tuukkanen, T. Hautala (2003) Adenoviral VEGF-A gene transfer induces angiogenesis and promotes bone formation in healing osseous tissues. J Gene Med *5:* 560–566.

Thor, A., V. Franke-Stenport, C.B. Johansson, L. Rasmusson (2007) Early bone formation in human bone grafts treated with platelet-rich plasma: preliminary histomorphometric results. Int J Oral Maxillofac Surg *36:* 1164–1171.

Vasconcelos Gurgel, B.C., P.F. Goncalves, S.P. Pimentel, G.M. Ambrosano, F.H. Nociti Jr., E.A. Sallum, M.Z. Casati (2007) Platelet-rich plasma may not provide any additional effect when associated with guided bone regeneration around dental implants in dogs. Clin Oral Implants Res *18:* 649–654.

Vogel, J.P., K. Szalay, F. Geiger, M. Kramer, W. Richter, P. Kasten (2006) Platelet-rich plasma improves expansion of human mesenchymal stem cells and retains differentiation capacity and in vivo bone formation in calcium phosphate ceramics. Platelets *17:* 462–469.

Wippermann, B., C. Donow, H.E. Schratt, F.C. den Boer, T. Blokhuis, P. Patka (1999) The influence of hydroxyapatite granules on the healing of a segmental defect filled with autologous bone marrow. Ann Chir Gynaecol *88:* 194–197.

Wittbjer, J., B. Palmer, K.G. Thorngren (1982) Osteogenetic properties of reimplanted decalcified and undecalcified autologous bone in the rabbit radius. Scand J Plast Reconstr Surg *16:* 239–244.

Yamada, Y., M. Ueda, T. Naiki, M. Takahashi, K. Hata, T. Nagasaka (2004) Autogenous injectable bone for regeneration with mesenchymal stem cells and platelet-rich plasma: tissue-engineered bone regeneration. Tissue Eng *10:* 955–964.

You, T.M., B.H. Choi, J. Li, J.H. Jung, H.J. Lee, S.H. Lee, S.M. Jeong (2007) The effect of platelet-rich plasma on bone healing around implants placed in bone defects treated with Bio-Oss: a pilot study in the dog tibia. Oral Surg Oral Med Oral Pathol Oral Radiol Endod *103:* 8–12.